Electronic structure and magnetic moments of $ZnO_{1-x}B_x$ with GGA and GGA+U

Yousif Shoaib Mohammed[1,2,3]

[1] Department of Physics, College of Science & Arts in Oklat Al-Skoor, Qassim University, Oklat Al-Skoor, Saudi Arabia
[2] Department of Physics, University of Dalanj, Dalanj, Sudan
[3] African City for Technology, Khartoum, Sudan

Abstract- Electronic structure and magnetic moments of (Boron) B-doped ZnO was investigated by ab initio electronic structure calculations based on the density functional theory (DFT) with the generalized gradient approximation (GGA). We also performed GGA+U calculations to further refine our results. It is found that single B atom at O site in ZnO becomes spin polarized with its many neighboring atoms with a total magnetic moment of 0.94 and 1.27 μB for GGA and GGA+U respectively. The magnetic coupling between doped B atoms is substantial leading to either antiferromagnetism or ferromagnetism with GGA+U. For the B-B distance is 7.942 Å by replacing two oxygen atoms at the opposite vertices of a ZnO wutizte. A strong antiferromagnetic coupling occurs.

Keywords - Magnetic moments; DOS;B; ZnO; supercell.

I. INTRODUCTION

Diluted magnetic semiconductors (DMSs) have attracted a great deal of attention because of the possibility of incorporating magnetic degrees of freedom in traditional semiconductors [1, 2]. DMSs are semiconductors which contain some magnetic atoms as impurities. They have the possibility to create functional material using the carrier control techniques in semiconductors. They are widely used in high- and low-tech applications such as anti-static coatings, touch display panels, solar cells, flat panel displays, heaters, defrosters, and optical coatings [3]. All these applications use transparent conductive oxides as simple passive electrical or optical coatings. ZnO is a direct bandgap semiconductor which is piezoelectric and has been used for transparent thin film transistors, blue and UV light-emitting diodes and laser diodes [4]. Recently ZnO attracts much attention because of its cheapness and abundance.

Interestingly, non-magnetic ion doped ZnO thin films also reveal robust ferromagnetism, e.g. nitrogen doped ZnO thin films (ZnO :N) [5, 6]. The mechanism behind the enhancement of ferromagnetism by the doped nitrogen is still unclear. Because of the completely filled d-orbits of the non-magnetic ion doped ZnO thin films, the origin of the ferromagnetism is out of the ordinary. Some researchers believe that the magnetic mechanism of non-magnetic ion doped thin films of transition metal oxide comes from the localized states of oxygen defects [7–9], which is different from the bound magnetic polaron (BMP) mechanism proposed by Coey [10] for magnetic ion doped transition metal oxides. Extensive studies have been carried out on ZnO based DMSs and there have been many reports of room temperature ferromagnetism in 3d TM doped ZnO DMSs [11-18]. Despite of these successes, however, there are disadvantages to use those magnetic TM impurities. On one hand, those 3d TM impurities tend to form small clusters or secondary phases in the host ZnO semiconductor which is detrimental for real applications. It has been straightly pointed out that there exist Co-O or Co-metal clusters in Co doped ZnO [11,12], which might be the origin of ferromagnetism in this system. The first-principles calculated results of Wang et al. also indicated that Cr in ZnO bulk tends to cluster around O and favors a ferromagnetic (FM) ground state [19]. Ferromagnetism was also reported in anumber of carbon systems [20-22]. Some of these studies have speculated that intrinsic carbon defects could be responsible for the observed magnetic properties. Carbon adatoms on carbon nanotubes [23] and carbon substitutional doping in boron nitride nanotubes [24] were predicted to induce magnetism in the respective systems.

From a physical/chemical point of view, ZnO is a very interesting material because of the mixed covalent/ionic aspects in the chemical bonding. ZnO crystallized in the hexagonal wurtzite structure (B4), which consists of hexagonal Zn and O planes stacked alternately along the c-axis. Anions and cations are fourfold coordinated like in the closely related zinc-blende structure. A tetrahedral coordinated bulk structure is typical for covalent semiconductors. On the other hand, ZnO shows great similarities with ionic insulators such as MgO [25]. This is why ZnO is often called the ‘‘ionic extreme’’ of tetrahedral coordinated semiconductors.

In this paper, we investigate the magnetic properties of $ZnO_{1-x}B_x$ DMS. The purpose of the present study is to give a guideline to synthesize new magnetic materials according to ab initio calculations.

II. COMPUTATIONAL METHODS

In this research, the possibility of fabricating wurtzite ZnO structure [26] based DMSs using non-magnetic dopant B is investigated using first principles calculations based on spin density functional theory (DFT) with the generalized gradient approximation (GGA) [27]. To simulate the ZnO1-xBx alloys, supercell approach was employed. We thus extended the original ZnO unit cell of four atoms [28] to a 2×2×2 supercell of 32 atoms, i.e., the unit cell size was doubled in all the three crystallographic axes. The supercell contains 16 molecules of ZnO. One and two of the 16 O atoms in the supercell was then substituted with B atoms. The substitution leads to an impurity concentration B of 6.25% and 12.5% respectively. All

calculations are carried out using the plane-wave VASP package [29-32]. The projector augmented wave (PAW) potentials [33] are used to represent the interactions between the valence electrons and the core. Since the 3d electrons on the transition metal atoms are presumably strongly correlated, the onsite Coulomb energy *U* was also taken into account with the so-called GGA+U scheme. The corresponding parameters *U* and *J* used for our calculations is *U-J* = 7 eV.

The electron wave function is expanded in plane-waves up to a cutoff energy of 360 eV, and the k points sampling with a mesh of points 7x7x3 generated by the scheme of Monkhost-Pack [34] ensured convergence accuracy. The Brich-Murnaghan EOS [33, 35] used to calculate the four parameters equation of states.

III. RESULTS AND DISCUSSION

Table 1, displays the calculated Lattice constants *a* and c, bulk modulus B_0, bulk modulus pressure derivative B_0', and cohesive energy *Ec* of wurtzite ZnO with GGA and GGA+U respectively. The values are determined by fitting the *P-V* data to the third-order Birch-Murnaghan [36] EOS. The table shows that when strong correlation is included, the lattice constant decrease, while the bulk modulus increase. Fig. 1, shows the computed lattice constants as a function of total energy for GGA and GGA+U respectively. From this figure we found that the GGA calculation is more stable than the GGA+U (see table 1).

Table 1: Lattice constant a and c, bulk modulus B_0, bulk modulus pressure derivative B_0', and cohesive energy Ec of wurtzite ZnO with GGA and GGA+U respectively. (c are in parenthesis).

Method	Type	*a* and c (Å)	B_0 (GPa)	B_0'	*Ec (eV)*	Reference
DFT	GGA	3.29 (5.37)	144.6	4.56	-	This work
	GGA+U	3.21 (5.24)	151.7	4.05	144.95	This work
DFT	LSDA	3.184(5.111)			-	20
DFT	GGA	3.28(5.29)			143.36	38
DFT	GGA	3.262(5.226)				45

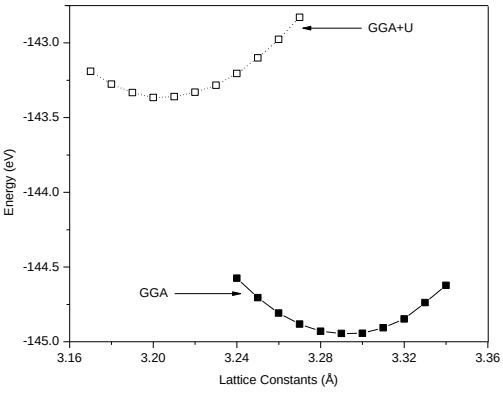

Fig. 1: Computed wurtzite ZnO lattice constants as a function of total energy for GGA and GGA+U respectively.

Fig. 2, shows ZnO (2x2x2) supercell in wurtzite structure containing 16 Zn and 16 O atoms. To study the magnetic effect of Boron (B) doped ZnO, we replaced one O atom (O8) with B atom which formed $Zn_{16}O_{15}B$ supercell, for the concentration B of 6.25%. Our spin-polarized calculation shows resultant total magnetic moments of 0.94 and 1.27 μB for GGA and GGA+U respectively. The GGA results is quite similar to that of Cu-doped ZnO (1.0 μB) [37] and N-doped ZnO (1.0 μB) [38, 39].

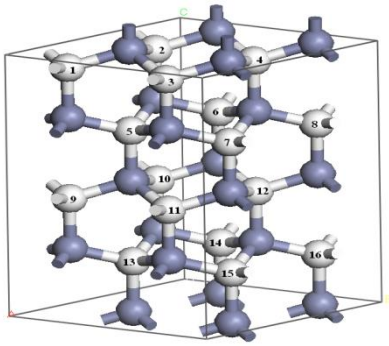

Fig. 2: (Color online) The (2x2x2) supercell of bulk ZnO wurtzite consisting of 16 Zn and 16 O atoms. The darker spheres are Zn. The numbered lighter spheres are O.

Fig. 3 shows the spin density distribution around the B atom for GGA and GGA+U respectively (larger for GGA+U). Most of the spin density in the B-doped ZnO is localized on the dopant itself and its 12 second-neighboring O atoms, with a minor contribution from the four nearest-neighboring Zn atoms. Therefore, the magnetic moment in B-doped semiconductors is mainly contributed by the anions, and it is resulted mainly from the delocalized 2*p* orbital. The B atom carries a magnetic moment of 0.331 and 0.49 μB for GGA and GGA+U respectively. The neighboring O atoms and Zn atoms have various magnetizations from 0.038 to 0.148 μB for GGA, while for GGA+U are ranged from 0.039 to 0.174 μB. This is quite different from the case of Mn doped GaN where the magnetization on atoms neighboring Mn is very small even though the Mn has a magnetization of 4 μB [40].

Table 2, shows the total magnetic moments, the spin polarized calculation of B atoms and of the *2p* electrons of the B atoms, and the total energy with GGA and GGA+U for concentration B of 6.25% respectively. From this table we found that the GGA is more stable than GGA+U calculation.

Table 2: Total magnetic moments (*Mtot*), the spin polarize calculation of B atom (*MB*), magnetic moments of *2p* electrons of the B atom (*M2p*), and the total energy (*Etot*) for concentration B of 6.25% with GGA and GGA+U respectively.

Type	*Mtot* (μB)	*MB* (μB)	*M2p* (μB)	*Etot* (eV)
GGA	0.94	0.331	0.315	-139.33
GGA+U	1.27	0.490	0.467	-136.40

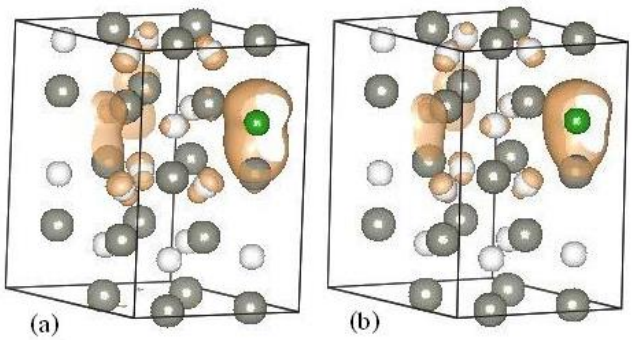

Fig. 3: (Color online) Spin density distribution around the one-B-atom doped ZnO in (a) GGA and (b) GGA+U respectively.

The total electronic DOS of ZnO and $Zn_{16}O_{15}B$ supercell, and the partial DOS of the 2*p* states of B atoms and of the second-nearest-neighboring O atoms and the 3*d* states of the four first-nearest-neighboring Zn atoms, for spin-up and spin-down electrons are plotted in Fig. 4 with GGA and GGA+U respectively. We note that the curves of DOS for spin-up and spin-down states are totally symmetric, and the Fermi level is located in the gap region, suggesting that ZnO is a semiconductor and nonmagnetic. We see that there is a significant change in the spin-up and spin-down total and partial DOS of the GGA compared to that of GGA+U.

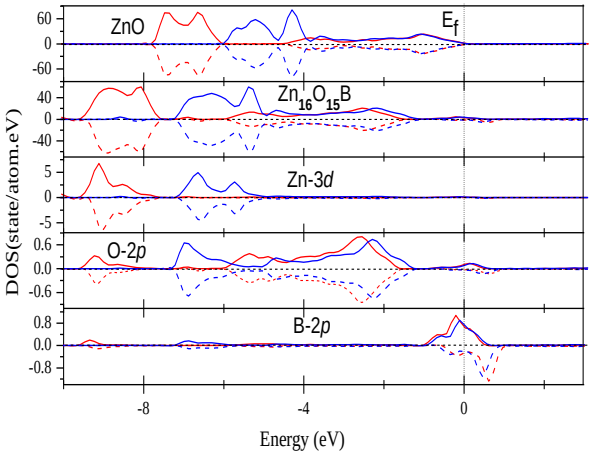

Fig. 4: (Color online) The total and partial DOS of B doped ZnO. Blue and red for GGA and GGA+U, solid and dotted lines for spin up and down respectively.

After understanding the local magnetic-moment formation in B-doped ZnO, we will go on to investigate the long-range coupling interaction of these magnetic moments. To investigate the magnetic coupling between B impurities, a pair of B atoms is incorporated into the same ZnO supercell by substituting two O atoms at sites marked Nos. (8, 6), (8, 5), and (8, 9) in Fig. 2 which are separated by 3.249, 5.628, and 7.942 Å respectively. This corresponds to a doping concentration of 12.5% B, which formed Zn16O14B2 supercell. In the first configuration B_{86}, B atoms cluster around Zn, namely, B-Zn-B. In the second B_{85}, the two B atoms are separated with the configuration of B-Zn-O-Zn-B, while in the last one B89, the two B atoms are separated with the configuration B-Zn-O-Zn-O-Zn-B along different directions.

The results of our calculations show that the magnetic moments of the two B dopants favor FM coupling in each of the three configurations with GGA. This verifies that the coupling between these two B atoms is FM as predicted by similar previous Cr-doped ZnO studies [41–43]. However, with the GGA+U a strong FM and antiferromagnetic (AFM) coupling takes place between the moments in each of the three configurations. The spin density distribution around the two B atoms of the (8, 5) structure is presented in Fig. 5, which shows the magnetic coupling between the two B ions separated by 5.628 Å. As can be seen, the near anions between impurity B atoms mediate the magnetic coupling. We believe that charge carriers localized around the anions between these B ions are polarized and have the same spin orientation as that of the B ions. Consequently, these polarized charge carriers mediate the long-range ferromagnetic coupling between the B ions [44].

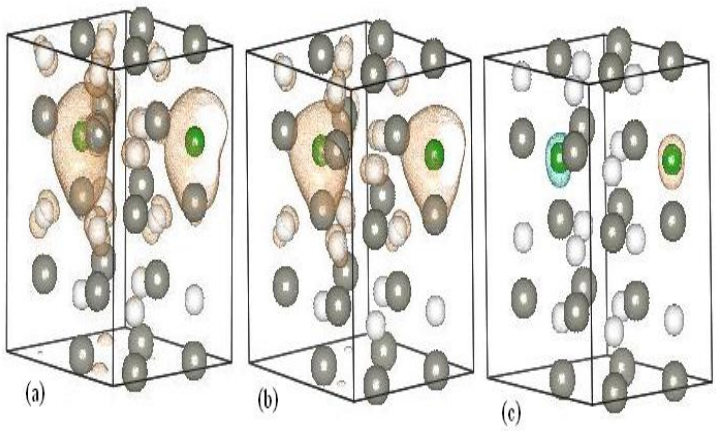

Fig. 5: (Color online) Spin density distribution around the B atoms for two-B-atom doped ZnO. For (a) FM GGA, (b) FM GGA+U, and (c) AFM GGA+U respectively.

Table 3, shows the total magnetic moments and the spin polarize calculation of two B atoms, magnetic moments of *2p* electrons of the two B atoms, and the total energy for the three different configurations of concentration 12.5% B with GGA and GGA+U respectively. Similar behaviors of B concentration of 6.25% are obtained. The table shows that the GGA+U preference for the AFM coupling in the three configurations are much stronger than that for the FM coupling and more stable. This suggests that with GGA+U the antiferromagnetism is possible as a new coupling in B-doped ZnO. The GGA+U energy difference between the FM and AFM phases, ($\Delta E = E^{AFM} - E^{FM}$) for the three configurations are shown in Table 4.

Table 3: Total magnetic moments (*Mtot*), the spin polarize calculation of B atoms (*MB*), magnetic moments of *2p* electrons of the B atoms (*M2p*), and the total energy (*Etot*) for concentration B of 12.5% with GGA and GGA+U respectively. (AFM values are in parenthesis).

	Type	*Mtot* (μB)	*MB* (μB)	*M2p* (μB)	*Etot* (eV)
Configuration a (d=3.249 Å)	GGA	1.54	0.281 0.281	0.267 0.267	-134.42
	GGA+U	2.16	0.429(0.483) 0.429(-0.483)	0.408(0.461) 0.408(-0.461)	-130.4402 (-130.4925)
Configuration b (d=5.628 Å)	GGA	1.54	0.280 0.280	0.266 0.266	-134.42
	GGA+U	2.16	0.429(0.483) 0.429(-0.483)	0.408(0.461) 0.408(-0.461)	-130.4409 (-130.4933)
Configuration c (d=7.942 Å)	GGA	1.49	0.283 0.270	0.270 0.257	-133.56
	GGA+U	2.35	0.464(0.528) 0.464(-0.528)	0.443(0.504) 0.443(-0.504)	-129.3823 (-129.4232)

Table 4: The GGA+U energy difference between the ferromagnetic (FM) and antiferromagnetic (AFM) phases $\Delta E = E^{AFM} - E^{FM}$.

	Configuration a (d=3.249Å)	Configuration b (d=5.628Å)	Configuration c (d=7.942Å)
ΔE (eV)	-0.0523	-0.0524	-0.0409

To visualize the changes in electronic structure and magnetic properties resulting from two-B doped ZnO. We plot the total and partial DOS corresponding to configuration *C*85 in Fig. 6. We note that there is a significant change in the spin-up and spin-down total DOS at the Fermi level in FM with GGA of $Zn_{16}O_{14}B_2$ compared to that with GGA+U. while the FM and AFM with GGA+U resulting in an asymmetric spin-up and spin-down DOSs. On the other hand, the main contribution to the moment comes from the B 2*p* orbitals. The spins of B 2*p* electrons are polarized and introduce new states near the Fermi level and magnetism does not result from Zn 3*d* orbitals [45].

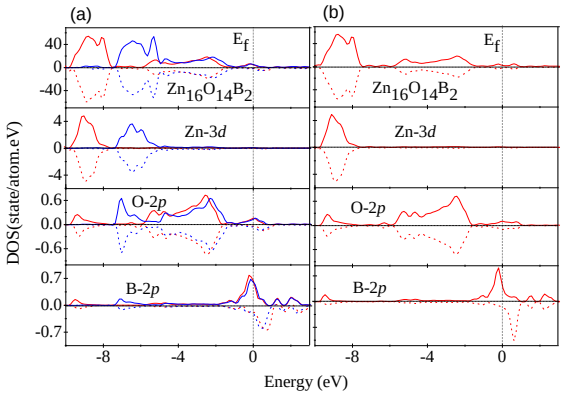

Fig. 6: (Color online) The total and partial DOS of two-B doped ZnO of (a) FM, and (b) AFM calculations. (blue for GGA, and red for GGA+U, Solid and dotted lines for spin-up and spin-down respectively.

IV. CONCLUSION

To our knowledge there is no experimental B-doped ZnO studies, so in the present work, we performed an extensive study of magnetic and electronic properties of B-doped ZnO. To this end, we have applied the GGA+U method to correct the electron structure. The main points of our study can be summarized as following:

1- Substitution of O by B in ZnO results in spin polarized state. Magnetization comes ubiquitously from atoms near the B atom.
2- The GGA calculations obtained only FM coupling.
3- When strong correlations are included, a new possible AFM coupling predicted, and the magnetic moments increased.

Therefore, B-doped ZnO with the new GGA+U AFM coupling may find possible applications in spintronics besides optoelectronics.

ACKNOWLEDGMENTS

I would like to thanks African City for Technology, Khartoum – Sudan so much.

REFERENCES

[1] J.K. Furdyna, *J. Appl. Phys.*, 1988, 64, pp. R29
[2] S.A. Wolf, D.D. Awschalom, R.A. Buhrman, J.M. Daughton, S. Von Molnar, M.L. Roukes, A.Y. Chtchelkanova, and D.M. *Treger, Science*, 2001, 294, pp. 1488.
[3] J.F. Wager, *Science*, 2003, 300, pp. 124.
[4] D.M. Bagnall, Y.F. Chen, Z. Zhu, T. Yao, S. Koyama, M.Y. Shen, and T. Goto, *Appl. Phys. Lett.*, 1997, 70, pp. 2230.
[5] N. H. Hong, J. Sakai, and V. Brize, *J. Phys.: Condens. Matter*, 2007,19, pp. 036219.
[6] C. F. Yu, T. J. Lin, S. J. Sun, and H. Chou, *J. Phys. D: Appl. Phys.*, 2007, 40, pp. 6497.
[7] J. M. D. Coey, *Solid State Sci*., 2005,7, pp.660.
[8] S. D. Yoon, Y. Y. Chen, A. Yang, T. L. Goodrich, X. Zuo, D. A. Arena, K. Ziemer, C. Vittoria, and V. G. Harris, *J. Phys.: Condens. Matter*, 2006, 18, pp. 355
[9] A. K. Rumaiz, B. Ali, A. Ceylan, M. Boggs, T. Beebe, and S. I. Shan, *Solid State Commun.*, 2007, 144, pp. 334.
[10] J. M. D. Coey, M. Venkatesan, and C. B. Fitzgerald, *Nature Mater.*, 2005, 4, pp. 173.
[11] K. Ueda, H. Tabata, and T. Kawai, *Appl. Phys. Lett.*, 2001, 79, pp. 988.
[12] J. H. Kim, J. B. Lee, H. Kim, D. Kim, Y. Ihm, and W. K. Choo, *IEEE Trans. Magn.*, 2002, 38, pp.2880.
[13] S. W. Lim, D. K. Hwang, and J. M. Myoung, *Solid State Commun.*, 2003, 125, pp. 231.
[14] J. Shim, T. Hwang, J. Park, S. J. Han, and Y. Jeong, *Appl. Phys. Lett.*, 2005, 86, pp. 082503.
[15] Y. W. Heo, M. P. Ivill, K. Ip, D. P. Norton, and S. Pearton, *Appl. Phys. Lett.*, 2003, 84, pp. 2292.
[16] P. Sharma, A. Gupta, K. V. Rao, F. J. Owens, R. Sharma, R. Ahuja, J. M. Osorio-Guillen, and G. A. Gehring, *Nat. Mater.*, 2003, 2, pp. 673.
[17] S. J. Han, J.W. Song, C. H. Yang, S. H. Park, J. H. Park, Y. H. Jeong, and K. W. Rhie, *Appl. Phys. Lett.*, 2002, 81, pp. 4212.
[18] Y. M. Cho, W. K. Choo, H. Kim, D. Kim, and Y. Ihm, *Appl. Phys. Lett.*, 2002, 80, pp. 3358.
[19] Q. Wang, Q. Sun, P. Jena, and Y. Kawazoe, *Appl. Phys. Lett.*, 2005, 87, pp. 162509.
[20] H. Pan, J. B. Yi, L. Shen, R. Q. Wu, J. H. Yang, J.Y. Lin, Y. P. Feng, J. Ding, L. H. Van, and J. H. Yin, *PRL*, 2007, 99, pp. 127201.
[21] S. Talapatra, P. G. Ganesan, T. Kim, R. Vajtai, M. Huang, M. Shima, G. Ramanath, D. Srivastava, S. C. Deevi, and P. M. Ajayan, *Phys. Rev. Lett.*, 2005, 95, 097201.
[22] H. Ohldag, T. Tyliszczak, R. Höhne, D. Spemann, P. Esquinazi, M. Ungureanu, and T. Butz, *Phys. Rev. Lett.*, 2007, 98, pp. 187204.
[23] P. O. Lehtinen, A. S. Foster, A. Ayuela, T. T. Vehviläinen, and R. M. Nieminen, *Phys. Rev. B*, 2004, 69, pp. 155422.
[24] R. Q. Wu, L. Liu, G. W. Peng, and Y. P. Fenga, *Appl. Phys. Lett.*, 2005, 86, pp. 122510.
[25] P.A. Cox, Transition Metal Oxides: An Introduction toTheir Electronic Structure and Properties, Clarendon Press, Oxford, 1992.
[26] R.W.G. Wyckoff, Crystal Structures, Vol. 1, 2nd Edition, Wiley, New York, pp. 112, 1986.
[27] J.P. Perdew, J.A. Chevary, S.H. Vosko, K.A. Jackson, M.R. Pederson, D.J. Singh, and C. Fiolhais, *Phys. Rev. B*, 1992, 46, pp. 6671.
[28] M. Usuda, N. Hamada, T. Kotani, and M. van Schilfgaarde, *Phys. Rev. B*, 2002, 66, pp. 125101.
[29] G. Kresse, and J. Hafner, *Phys. Rev. B* , 1993, 47, pp. 558.
[30] G. Kresse, and J. Joubert, *Phys. Rev. B*, 1999, 59, pp. 1758.
[31] G. Kresse and H. Hafner, *Phys. Rev. B*, 1994, 48, pp. 13115.
[32] G. Kresse and J. Fürthmüller, *Comput. Mater. Sci.*, 1996, 6, pp. 15.
[33] F. Brich, *Geophys. Res.*, 1951, 57, pp.129.
[34] M. Methfessel, and A. T. Paxton, *Phys. Rev. B*, 1989, 40, pp. 3616.
[35] F. D. Murnaghan, *Proc. Natl Acad. Sci. USA*, 1944, 30, pp. 244.
[36] J. R. Macdonald and D. R. Powell, *J. Res. Natl. Bur. Stand., Sect.*, 1971, A 75, pp. 441.
[37] L. H. Ye, A. J. Freeman, and B. Delley, *Phys. Rev. B*, 2006, 73, pp. 033203.
[38] Q. Y. Wu, R. Wu, Z. G. Chen, Y. B. Lin, J. M. Zhang, and Z. G. Huang, *INEC*, 2008, pp.700.
[39] L. Shen, R. Q. Wu, H. Pan, G. W. Peng, M. Yang, Z. D. Sha, and Y. P. Feng, *Phys. Rev. B*, 2008, 78, pp. 073306.
[40] B. Sanyal, O. Bengone, and S. Mirbit, *Phys. Rev. B*, 2003, 68, pp. 205210.
[41] K. Sato and H. K. Yoshida, Jpn. *J. Appl. Phys.*, 2000, 39, pp. L555.

[42] E. Kulatov, Y. Uspenskii, H. Mariette, J. Cibert, D. Ferrand, H. Nakayama, and H. Ohta, *J. Supercond.*, 2003, 16, pp. 123.
[43] Y. Uspenskii, E. Kulatov, H. Mariette, H. Nakayama, and H. Ohta, *J. Magn. Magn. Mater.*, 2003, 258-259, pp.248.
[44] P. J. Hay, J. C. Thibeault, and R. Hoffmann, *J. Am. Chem. Soc.*, 1975, 97, pp. 4884.
[45] Q. Wang, Q. Sun, G. Chen, Y. Kawazoe, and P. Jena, *Phys. Rev.*, 2008, B 77, pp. 205411.

AUTHOR

Corresponding Author:

Yousif Shoaib Mohammed

(Assistant Professor of Computational Physics) received the B.Sc in Physics from Khartoum University – Oudurman – Sudan (1994) and High Diploma in Solar Physics from Sudan University of Science and Technology – Khartoum – Sudan (1997) and M.Sc in Computational Physics (Solid State – Magnetism) from Jordan University – Amman – Jordan and PhD in Computational Physics (Solid State – Magnetism – Semi Conductors) from Jilin University – Changchun – China (2010). He worked at Dalanj University since 1994 up to 2013 and worked as Researcher at Africa City of Technology – Khartoum – Sudan since 2012. Then from 2013 up to now at Qassim University – Kingdom of Saudi Arabia (E-mail: yshm@yahoo.com).